Gas vesicle protein expression for reconstitution of synthetic gas vesicles in yeast

Harin Jung [1,2,3,4], Hua Ling [1,2,3,4], Yong Quan Tan [1,2,3,4], Nam-Hai Chua [1,2,3,4,5] Wen Shan Yew [1,2,3,4], Matthew Wook Chang [1,2,3,4]*

[1]NUS Synthetic Biology for Clinical and Technological Innovation (SynCTI), National University of Singapore, Singapore;
[2]Synthetic Biology Translational Research Programme, Yong Loo Lin School of Medicine, National University of Singapore, Singapore;
[3] Department of Biochemistry, Yong Loo Lin School of Medicine, National University of Singapore, Singapore;
[4] Wilmar-NUS Corporate Laboratory, National University of Singapore, Singapore;
[5] Temasek Life Sciences Laboratory, Singapore;

* Correspondence: bchcmw@nus.edu.sg; +65 6601 3687

Abstract: Given the potential applications of gas vesicles (GVs) in multiple fields including antigen-displaying and imaging, heterologous reconstitution of synthetic GVs is an attractive and interesting study that has translational potential. Here, we attempted to express and assemble GV proteins (GVPs) into GVs using the model eukaryotic organism *Saccharomyces cerevisiae*. We first selected and expressed two core structural proteins, GvpA and GvpC from cyanobacteria *Anabaena flos-aquae* and *Planktothrix rubescens*, respectively. We then optimized the protein expression conditions and validated GV assembly in the context of cell flotation and GV shapes. We found that when two copies of AnaA were integrated into the genome, it resulted in cell floatation and GV production regardless of GvpC expression. Next, we co-expressed chaperone-RFP with the GFP-AnaA to aid the AnaA aggregation. The co-expression of individual chaperones (Hsp42, Sis1, Hsp104, and GvpN) with AnaA led to the formation of larger inclusions and enhanced the sequestration of AnaA into the perivacuolar site. To our knowledge, this represents the first study on reconstitution of GVs in *S. cerevisiae*. Our results could provide insights into optimizing conditions for heterologous protein expressions as well as the reconstitution of other synthetic microcompartments in yeast.

Keywords: Gas vesicle; Gas vesicle protein; Protein aggregation; Cellular aging; Spatial protein quality control; yeast

36

1. Introduction

Gas vesicles (GVs) are gas-filled proteinaceous intracellular compartments found in several microbes such as cyanobacteria. GVs are observed as spindle- and cylindrical-shapes which form small bicone structures which then extend to develop as mature GVs. GVs increase cellular buoyancy thus facilitating the upward movement in water columns [1].

The wall of GV is primarily formed by extremely high hydrophobic GV protein A or B (GvpA/B, 7-8 kDa), which is attached to the GvpC in some species to strengthen the GV structure. Specifically, an NMR study shows that the secondary structure of GvpA contains two α-helix separated by two antiparallel β-sheets forming an asymmetric dimer via its β-sheets of GvpA. This leads to the formation of GvpA aggregates that consist of the rib structure of the GV [2, 3]. GvpC is larger and diverse in size which depends on the number of highly conserved 33-amino acid repeat regions (33-RRs), forming up to five tandem repeats [1, 4]. The 33-RRs are thought to allow periodic interaction of GvpC with the ribs formed by GvpA [5], correlated with the strength and dimension of GVs [6]. Besides Gvp A/B and GvpC, there are other 6-12 protein factors that are either responsible for the GV assembly process or small components of the GV wall in native GV producers. Due to the aforementioned properties of GVPs, GVP structure and the mechanism on GV assembly are yet to be fully elucidated.

Recently, potential uses of GVs as a genetically encodable acoustic reporter (subcellular microcompartment) for detecting ultrasound [7] and magnetic resonance imaging (MRI) [8] have gained significant attention. Several studies have demonstrated that the reconstitution of GVs gives a higher ultrasound contrast in *E. coli*, *Salmonella typhimurium* [9], and the mammalian cell [10]. In many of these cases, multiple GVPs are required to successfully reconstitute GVs. For instance, for robust expression of GVPs, one major structural GVP and 8 accessory GVPs (of which six GVPs should be further supplemented as a booster [10]) are required to enable the efficient reconstitution of GVs in mammalian cells. Two recent studies have demonstrated the reconstitution of synthetic GVs by co-expressing only two core GVPs, i.e. GvpA and GvpC [11, 12]. Despite such successes, it is challenging to effectively reconstitute GVs in heterologous systems, which is likely due to non-specific aggregation of GvpA [3, 13, 14].

In this study, we aimed to express GVPs and reconstitute synthetic GVs in yeast *S. cerevisiae*. We first selected and optimized the expression of four core GVP genes from cyanobacteria *Anabaena flos-aquae* (Ana) and *Planktothrix rubescens* (Pla) (AnaA, AnC, PlaA, and PlaC) respectively, and validated GV assembly in the context of cell flotation

and GV shapes. Next, we co-expressed chaperones (Hsp42, Ydj1, Sis1, Sse1, Ssa1 and Hsp104) respectively with the GFP-AnaA to aid the inclusion formation of AnaA aggregates. To our best knowledge, this is the first study to reconstitute GVs in *S. cerevisiae*. Our study could provide insights into the expression and sequestration of heterologous proteins as well as the reconstitution of other synthetic microcompartments in yeast.

2. Results

2.1 Heterologous expression of gas vesicle proteins

We synthesized *gvpA* and *gvpC* genes of two cyanobacteria, *Anabaena flos-aquae* and *Planktothrix rubescens* respectively with codon optimized for yeast *S. cerevisiae*, and named them AnaA, AnaC, PlaA and PlaC as shown in Table 1.

Table 1. List of genes in this study.

Protein	Description	UniProt ID
AnaA	GvpA of *Anabaena flos-aquae*	P10397
AnaC	GvpC of *Anabaena flos-aquae*	P09413
PlaA	GvpA of *Planktothrix rubescens*	P0A3G1
PlaC	GvpC of *Planktothrix rubescens*	Q9R461
GvpN	GvpN of *Anabaena flos-aquae*	P55150
Hsp42	Small heat shock protein	Q12329
Ydj1	Type I HSP40 co-chaperone	P25491
Sis1	Type II HSP40 co-chaperone	P25294
Sse1	Adenyl-nucleotide exchange factor (NEF)	P32589
Ssa1	Hsp70 family ATPase	P10591
Hsp104	Hsp100 disaggregase	P31539

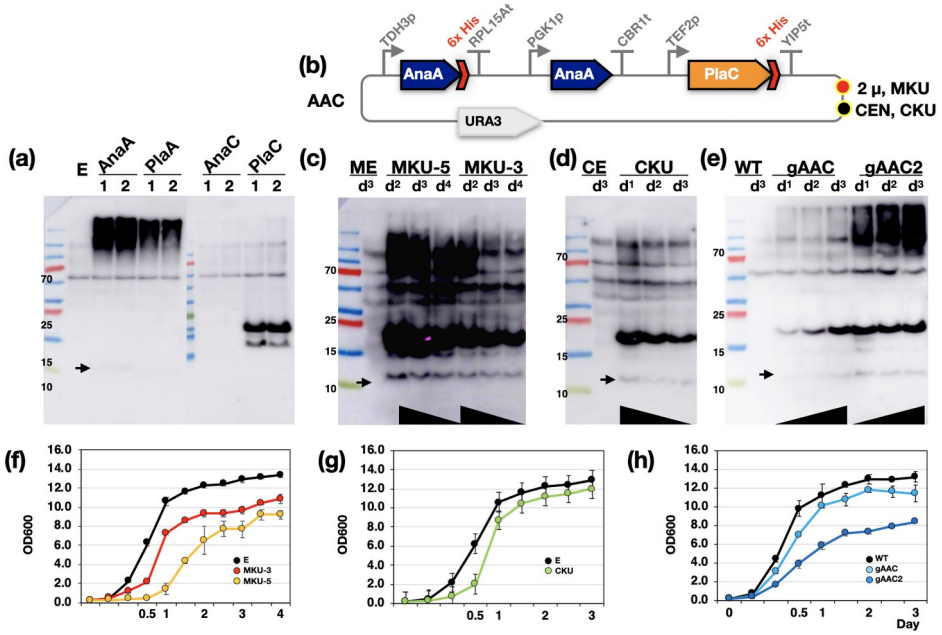

Figure 1. Comparison of the gas vesicle protein expression and cell growth between in the plasmid and by the genomic integration. **(a)** Western blot analysis of GvpAs (AnaA and PlaA) and GvpCs (AnaC and PlaC) of *A. flos-aquae* (Ana) and *P. rubescens* (Pla). **(b)** Schematic diagram of MKU (ori 2 micron) and CKU (ori CEN) plasmids carrying one copy of *AAC* gene. AAC was integrated into the genome to generate yeast strains carrying one copy (gAAC) and two copies (gAAC2) of AAC in the genome. **(c-e)** Western blot analysis of GVP expression based on MKU (c) and CKU (d) plasmids and genome integration (gAAC and gAAC2) **(e)**. Arrow indicates the band of GvpA dimer. The accumulation of GVPs was indicated with a black triangle on the bottom of each blots. **(f-h)** Representative growth profiles of MKU **(f)**, CKU **(g)**, gAAC, and gAAC2 **(h)** strains. Values shown are the mean of three independent experiments. Error bar indicates one standard deviation.

Each GvpA and GvpC gene was cloned with DNA sequences encoding 6×His-tag and expressed under the control of yeast constitutive promoters, P_{TDH3} and P_{TEF2}, respectively using a Golden-Gate assembly expression system derived from YeastFab [24]. Four plasmids were transformed into yeast cells and both GvpA and GvpC proteins were detected mainly in the insoluble fractions by Western blot analysis (Figure 1a). AnaA expression was approximately two times higher than PlaA, apart from PlaC which was also successfully expressed. However, AnaC expression was not observed, which could be due to the presence of five highly conserved 33-RRs, comprising of high glutamic acid (Q), alanine (A) and glutamine (G) of AnaC protein (Figure 1a and S1c). GvpA were detected at the top and bottom of the Western blot, respectively (Figure 1a, arrow), in line with previous observations that GvpA proteins aggregates cannot be dissolved even in the presence of SDS. In order to further verify the expression of AnaA, PlaA, AnaC, and PlaC, we constructed yeast strains that carried the plasmid with two copies of GvpAs and one copy of GvpC (Figure S2a), in line with the GvpA to GvpC ratio in the natural Ana-GV [1].

Among these strains, we observed the expression of both GvpA and GvpC only in the MKU2 transformants comprising AnaA and PlaC (Figure S2b). Therefore, we selected the combination of AnaA and PlaC (AAC) for further analysis (Figure 1b).

To determine an optimal condition for AAC protein expression and cell growth, we compared AAC expression levels and growth profiles from different copy numbers of AAC genes in plasmids and the genome. Specifically, we performed plasmid-based expression at high copy (2-micron ori, MKU) and low copy (CEN ori, CKU). Next, we integrated AAC genes into a single locus (gAAC) and two loci (gAAC2) (Figure 1b-h). We observed that the amount of AAC proteins decreased with cell growth in the plasmid-based strains. In comparison, AAC protein expression increased along with cell growth in the genome integration-based strains (Figure 1c-h). In particular, Figure 1c shows that two independent transformants of MKU (MKU-5, MKU-3) had different levels of AAC expressions, and the accumulation of ACC decreased along with cell growth from day 2 to day 4, which represents inconsistent level of AAC expression in different transformants from the 2-Micron-based expression system. The accumulation of ACC proteins in a CKU transformant also decreased along with cell growth (Figure 1d). By contrast, the accumulation of ACC proteins with genome integrations (Figure 1e) increased along with cell growth, where gAAC2 gave a higher expression than gAAC. Furthermore, we noted that there was more severe growth defect when the AAC expression level was higher. Particularly, MKU-5 had higher expression of AAC proteins, resulting in more severe growth defects than MKU-3 (Figure 1c and f). Amongst the tested AAC-expressing strains, both gAAC and gAAC2 showed the accumulation of AAC proteins and relatively less growth defect than that from the plasmid-based expression. Therefore, the genome integration-based expression is more suitable for GVP expression than the plasmid-based expression, which could be attributed to the consistency of AAC copy number in the genome. The genome integration-based expression was selected to validate GV assembly.

2.2 Validation of GV assembly

Using the abovementioned genome integration strategy for GVP expression, we constructed a set of GVP strains integrated with gC, gA, gAA, gAAC and gAAC2 into the genome as shown in Figure 2a. Next, we confirmed cell growth and the GVP expressions (Figure S3) and evaluated GV formation (Figure 2). Cell floatation is a phenotype of GV assembly causing cell buoyancy. Therefore, GV formation can be evaluated by a cell floating assay. To perform the cell floating assay, we set up a specific condition to compare the

sedimentation velocity between the GVP strains and wild-type (WT) control. Figure 2b shows that gAA and gAAC2 cells exhibited floating features displayed by dispersed cells (day 2 and day 3) while the others such as gC and gA cells sunk and formed a clear boundary like a WT control, suggesting GV formation in gAA and gAAC2 cells and the resulting in buoyancy. Interestingly, gAAC cells did not exhibit the floating phenotype, which might be due to the improper assembly of GVPs into GVs. The results of the cell floating assay indicate that both gAA and gAAC2 cells contained the reconstituted GVs.

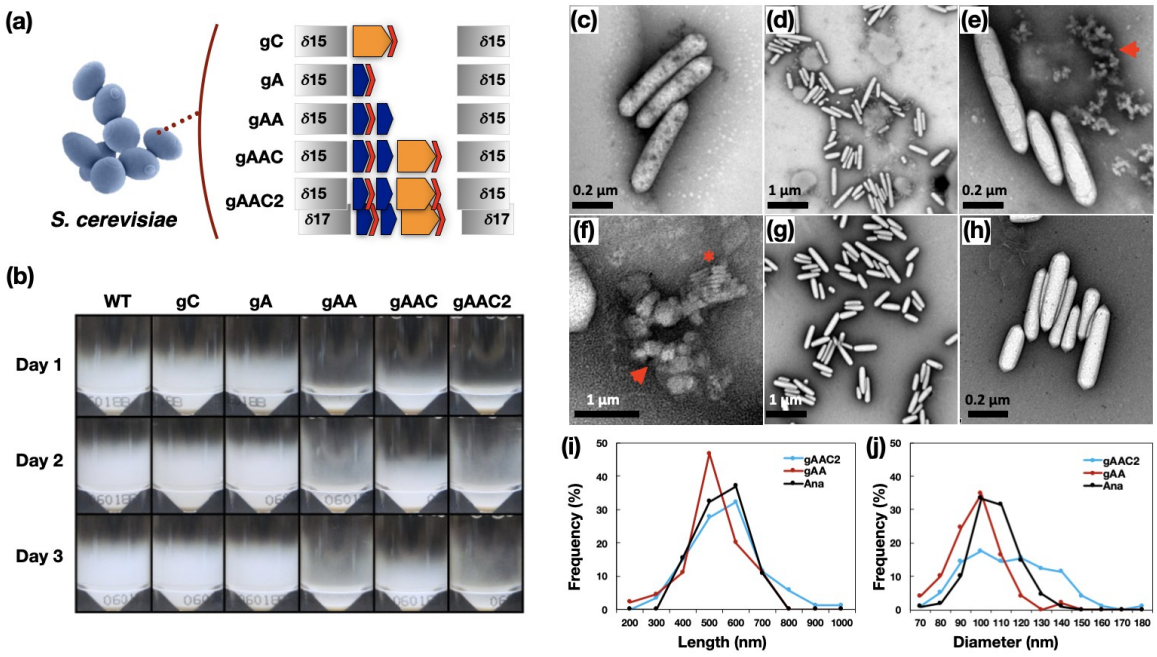

Figure 2. Floating assays of yeast cells expressing GVPs integrated into the genome, GV observation, and dimension. **(a)** Representative diagram of the designated genome integrated GVP strains. **(b)** The cell floating assay observing different sedimentation velocity of the genome integrated GVP strains. **(c-h)** TEM images of GVs isolated from the gAA **(c)** and gAAC2 **(d-f)** strains and the *Anabaena flos-aqua*e (AnaGV) **(g and h)** as a control. Red arrow and asterisks indicate amorphous protein aggregates and structured protein aggregates, respectively **(e and f)**. Diameter **(i)** and length **(j)** of GVs on TEM images were measured by using ImageJ. n = 87, 138 and 108 for gAA_GV, gAAC2_GV, and AnaGV, respectively.

To confirm the reconstitution of GVs in gAA and gAAC2 cells, we isolated GVs and observed them using a transmission electron microscope (TEM). TEM results show GVs in a typical shape with biconical ends in a long cylinder as observed from both gAA (Figure 2c) and gAAC2 cells (Figure 2d and e), which is similar in appearance to native AnaGV (Figure 2g and h). We noted that GVs from gAA, gAAC2 and AnaGV displayed similar distributions in length to each other, but different distributions in diameter, especially in the gAAC2 strain. Specifically, GVs with the diameter of 90-120 nm accounted 61.9% in gAAC2, less than 79.6% in gAA and 89.8% in Ana, respectively. GVs with a bigger

diameter (> 120 nm) accounted 30.0% in gAAC2, more than 2.0% in the gAA and 5.6% in Ana (Figure 2i and j). Such differences in the distribution of the diameter suggest that PlaC likely affected the diameter GVs of gAAC2 through its interaction with AnaA. We also observed that the GVs isolated from gAA and gAAC2 were attached to each other through the side of the cylinder (Figure 2d and e), similar to the features of GV clusters cylindrical stacking that was observed inside *Anabaena flos-aqua*e (Figure 2g and h) [26]. In addition, we observed lots of amorphous protein aggregates and relatively structured aggregates from the gAAC2 strain (Figure 2e and f). The cell flotation and GVs observed by using TEM confirm the successful assembly of GVs in the engineered yeast cells.

2.3 Chaperone-aided GVP aggregation

It is known that the formation of appropriate GvpA aggregates is instrumental for the GV assembly, and the rapid GV assembly is critical for the maintaining of cell viability in terms of the protein homeostasis in most GV production microorganism [2, 3, 27]. We hypothesized that the elucidation of GVP aggregates and optimization of GVP accumulation by co-expressing chaperones involved in a spatial protein quality control would be critical for the GV assembly.

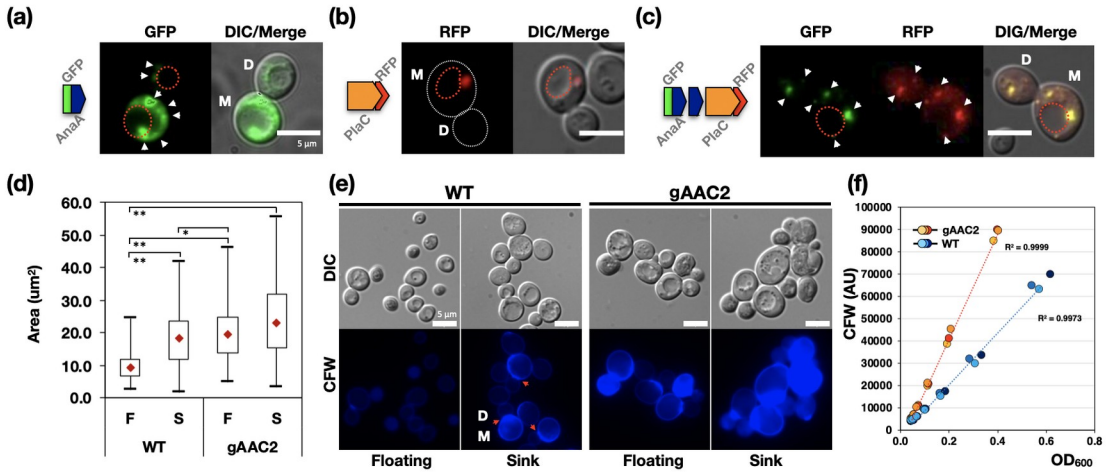

Figure 3. Analyses on the aggregates of AnaA and PlaC and the aggregates-related phenotypes. **(a-c)** Fluorescence microscopic analysis of AnaA and PlaC aggregates in the yeast cell harboring a plasmid of GFP-AnaA **(a)**, PlaC-RFP **(b)** and both GFP-AnaA and PlaC-RFP based on genome integration **(c). (d)** The cell size represented by cell area. The areas are shown in the box plot. The upper and lower lines of each box indicate 75% and 25% of all. Red diamond indicates a median. F, floating population and S, sink population. **(e)** Microscopic analysis on the floating and sink cells of WT control and gAAC2. Cells were observed under a microscope with DIC and DAPI filter to detect the fluorescence of CFW used for staining of yeast cell wall. **(f)** Quantitated CFW fluorescence intensity of WT control and gAAC2 cells against the cell density (OD_{600})

along with their growth. Values are three independent experiments and means are presented with dotted lines. White arrow indicates GFP-GvpA aggregates, red dotted circle indicates vacuole, and red arrow indicates septum. Single (*P < 0.05) and two asterisks (**P < 0.01) represent significant differences by the Student's t-test between the indicated populations.

First, to confirm the formation of AnaA and PlaC aggregates, we expressed AnaA, PlaC, or both, which was fused with fluorescent reporter proteins (GFP and RFP, respectively), observed and compared their foci formed in the yeast cells. Specifically, we constructed yeast strains expressing fusion proteins GFP-AnaA (Figure 3a), PlaC-RFP based on plasmids (Figure 3b) and co-expressing GFP-AnaA and PlaC-RFP based on the genome integration (Figure 3c). Our microscopic results show that GFP-AnaA formed multiple foci in both parental (M) and daughter cells (D) while PlaC-RFP formed a single inclusion in a parental cell (Figure 3a and b). Interestingly, both GFP-AnaA and PlaC-RFP formed multiple foci in both M and D cells when they were co-expressed, likely due to interaction of the two proteins with each other (Figure 3c). We speculate that the GFP-AnaA present in D cells was obtained from M cells during cell division, suggesting impaired asymmetric cell division. The microscopic observation (Figure 3a-c) also suggests that the size of D cells was increased and comparable to M cells when only GFP-AnaA, or both GFP-AnaA and PlaC-RFP were expressed. To further confirm the increase in cell size, we compared the cell size by measuring the cellular area of the floating and the sink cells of gAAC2 over WT cells. Our comparison shows that the cellular areas of gAAC2 were at 2.1 (floating cells) and 1.3 times (sink cells) larger than those of WT, respectively (Figure 3d). We also found that the gAAC2 cells had higher calcofluor white (CFW) fluorescence intensity (Figure 3e and f) than WT cells, suggesting that gAAC2 cells had a thicker cell wall than WT cells [28]. Given the slow growth (Figure 1h) and the increase in cell size and cell wall thickness of gAAC2, we speculate that cellular aging was accelerated in the gAAC2 strain mainly due to the inappropriate accumulation of GVP aggregates.

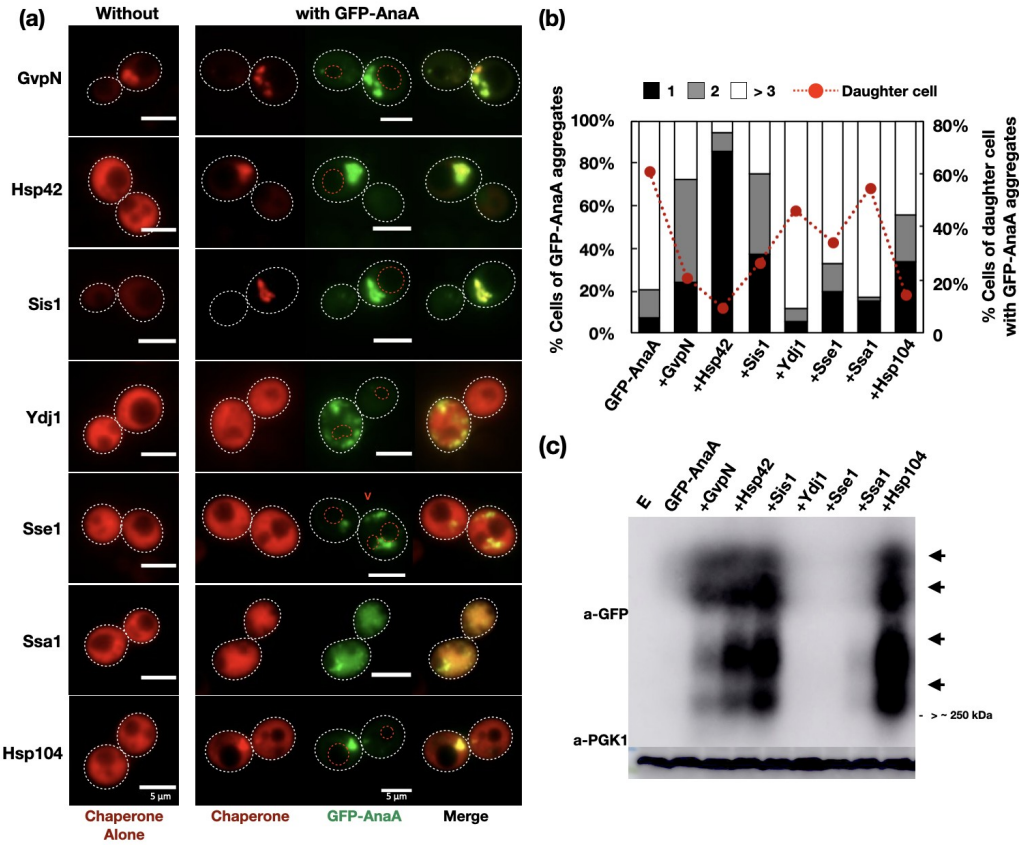

Figure 4. Spatial sequestration of GFP-AnaA aggregates by co-expressing respective chaperons in yeast. **(a)** Fluorescence microscopic analysis on the yeast cells expressing each chaperon-RFP without (panel "without") and co-expressing with the GFP-AnaA (panel "with GFP-AnaA"). **(b)** Proportion of cells with various numbers of inclusions of GFP-AnaA aggregates (left axis) and daughter cells (right axis) expressing GFP-AnaA and co-expressing chaperone-RFP with indicated chaperones. n = ~100 in each strain. The red dotted circle indicates vacuole. **(c)** Western blot analysis on GFP-AnaA protein aggregates at high molecular weight using anti-GFP (a-GFP) and anti-PGK1 (a-PGK1) separated on the semi-denaturing detergent agarose gel electrophoresis (SDD-AGE). PGK1 was used an internal reference protein. The arrow heads indicate different sizes of GFP-GvpA aggregates.

We turned to co-expression of chaperones to aid the appropriate accumulation of GVP and reduce formation of protein aggregates [17]. Specifically, we chose and expressed 6 individual chaperones (Hsp42, Sis1, Ydj1, Sse1, Ssa1 and Hsp104) endogenous to *S. cerevisiae* and one GV accessary protein (GvpN) predicted to function as a molecular chaperone [29]. Next, we compared the number of foci of GFP-AnaA aggregates with and without chaperone-RFP in the yeast cells (Figure 4a and b). The data indicates that when the cells having each chaperone was expressed alone (Figure 4a), there was a significant reduction of diffused cytosolic chaperones in cells with Hsp42, Sis1, Hsp104, and GvpN when co-expressed with GFP-AnaA (Figure 4a, right panel). These changes were accompanied by the accumulation of larger inclusions of GFP-GvpA composed of multiple

aggregates to the perivacuolar site. However, the expression of the other chaperones (Ydj1, Sse1, and Ssa1) only generated small multi-foci of GFP-AnaA aggregates that are either similar to (Ydj1, and Sse1) or much smaller (Ssa1) than that of GFP-GvpA expressed alone. These results suggest that these chaperones (Hsp42, Sis1, Hsp104, and GvpN) are likely to interact with GFP-AnaA aggregates and sequester them into the perivacuolar site. These strains exhibited significantly reduced proportion of GFP-GvpA aggregates in D cells from 80% to 10%, approximately (Figure 4b). Also, denaturing detergent polyacrylamide gel electrophoresis (SDD-PAGE) results confirmed the presence of large aggregates in the strains co-expressing GFP-AnaA with four respective chaperones (Hsp42, Sis1, Hsp104, and GvpN) (Figure 4c), which is in agreement with our microscopic observations in Figure 4a. The inclusion formation of GFP-GvpA aggregates which are docked near the perivacuolar site likely suggests the restoration of the asymmetric cell division that was impaired in the GFP-AnaA strain without the co-expression of chaperones. Given the enhancement of the inclusion formation and sequestration of GvpA aggregates near the perivacuolar site, we speculate the improvement of GVP accumulation and GV assembly by co-expressed chaperones, and it is likely to improve the appropriate aggregation of GVPs and GV assembly through co-expressing the four respective chaperones in the gAAC2 strain.

3. Discussion

Various attempts have been made to reconstitute GVs in various organisms such as *Halobacterium* species [30], *E. coli* [31, 9], and mammalian cells [10], in which multiple genes of the *gvp* operon are required for the GV assembly. Recently, two structural proteins, GvpA and GvpC of *P. rubescens* were expressed for reconstituting GV in *E. coli* and mammalian cells [11, 12]. In these studies, although the cell floating performance and MRI contrast have been validated, respectively, there is lack of sufficient elucidation of GV properties, and there is a severe growth defect likely resulting in low cell viability and poor GV production. To our knowledge, there has been no study on the genetic constitution of GVs in *S. cerevisiae* where the genetic manipulation and expression of heterologous proteins are well established. Therefore, we engineered *S. cerevisiae* to express GVPs and evaluated GV assembly. In this study, we observed the growth defect which is dependent on the copy number of AAC in GVP yeast strains through comparing the AAC expression levels and cell growth between plasmid- and genome integration-based expressions (Figure 1). In the Western blot analysis, AnaA protein was detected as aggregates at different sizes,

and PlaC protein was detected as a band at a single size. Different sized aggregates and large inclusions can be formed when misfolded proteins fail to refold [32]. The formation of such differentiated protein aggregates is a hallmark of aging and proteotoxic stress [33]. In addition, we observed that GFP-AnaA formed multiple foci (Figure 3a), compared to PlaC-RFP which formed a single inclusion (Figure 3b). Smaller aggregates are known to be more harmful to cell fitness than larger inclusions [34]. Hence, we posit that the growth defects of the GVP strains are primarily due to the inappropriate aggregation of GvpA protein.

Cell floatation in cyanobacteria is a complex phenomenon that is affected by several factors including cell cycle, cell wall hydrophobicity, and genetic and environmental factors [35, 36, 37]. The presence of GVs inside the cells might contribute to cell buoyancy, which is supported by the cell floatation performance exhibited in gAA and gAAC2 cells (Figure 2b). Interestingly, the flotation of GVP strains was observed only after cells were cultured for at least 2d (the 1st cultivation), diluted with fresh medium and then cultured under stationary condition for 1d (the 2nd cultivation). Under such a specific condition, we reasoned that the second cultivation using the fresh medium resulted in the relatively higher production of CO_2 and its permeation into the GV so that to facilitate the cell floatation. Therefore, the cell floating of GVP yeast strains is subject to the amount of gas surrounding the yeast cells in addition to the properties of GVs (e.g., number, size and shape) and the yeast cells (e.g., cell size and cell wall thickness).

Consistent to the typical shape of the AnaGV (Figure 2g and h), our results prove either only AnaA or both AnaA and PlaC are able to form GVs appearing in a typical shape and stacking property of natural GVs [26], even though these gas vacuole proteins originated from different species. However, in contrast to those of the gAA strain, the diameter of GVs isolated from the gAAC2 strain has a broader range, likely due to the structural difference determined by the protein sequence of PlaC [1, 38]. In particular, AnaC is composed of five highly conserved 33-RRs while PlaC has less conserved and incomplete three repeat regions (Figure S1c). Such differences in the protein sequence of PlaC may result in incomplete interactions with the AnaA cylinder, resulting in GVs with a wider range of diameters. Such interactions between AnaA and PlaC are also supported by the change in GvpC-RFP distribution from a single inclusion without the co-expression of GFP-AnaA to several multiple foci with the co-expression of GFP-AnaA (Figure 3b and c).

Specific cell size is important for cellular function, and changes in cell size are often observed during the yeast cellular aging, or cells under pathological conditions such as cancer [39]. According to a recent study, the DNA content of the oversized cell does not

change, leading to cytosolic dilution and consequently cell cycle arrest. Such changes may result in the impairment of gene transcription and translation, and subsequently weaken overall cellular functions [40]. In this study, the increased cell size and thicker cell wall of the GVP strain (Figure 3d-f) with the slower cell growth suggest cellular aging, which seems to be exacerbated along with the repeated enrichment of the floating population. We found the gradual disappearance of cell flotation performance till the 5th subculture (data not shown), longer than 8-15 generations reported for the natural occurrence of the typical cellular aging [41]. Such instability of the cell flotation likely in relation to cellular aging also suggests unstable GVP expressions and the GV assembly, which partially explains the presence of plenty aggregates and inconsistency of GV production in the GVP yeast strains (Figure 2e and f).

Numerous studies have reported that misfolded protein aggregates are cytotoxic and may promote cellular aging, represented by the increased cell size [33, 42, 43]. The misfolded proteins and protein aggregates are processed by several molecular chaperones in the cells [44]. As most plentiful chaperone, Hsp70-type chaperones are instrumental for protein refolding and quality control [21, 45]. For the protein refolding in yeast cells, Hsp70 chaperones (Ssa1 and Ssa2) form a network with a Hsp40 co-chaperone (Ydj1) and the nucleotide exchange factor (NEF) (Sse1), then facilitating refolding [20]. For the protein disaggregation, Hsp70 recruits and activates the Hsp104 during the aggregation initiating events [19]. In our study, the co-expression of Ydj1, Sse1 and Ssa1, respectively didn't result in larger inclusions of GFP-AnaA aggregates in yeast cells, suggesting this misfolded GFP-AnaA aggregates were processed neither by the refolding machinery nor by the disaggregation. In contrast, GFP-AnaA aggregates formed larger inclusions and recovered the asymmetric cell division upon the co-expression of Hsp42, Sis1 and Hsp104 (Figure 4a-c), agreeable to their known functions such as facilitating the inclusion formation of the cytosolic protein aggregates and sequestrating these inclusions into specific sites [21, 45, 46]. Based on these results, we speculate that GFP-GvpA aggregates were sequestrated into the specific site near the vacuole such as IPOD aided by Hsp42, Sis1, and Hsp104. The sequestration likely resulted in a recovery of the asymmetric cell division by Hsp42, Sis1 and Hsp104 which are implicated in the curing function of the yeast prion [PSI^{+}] that is an amyloid form of Sub35 serving as a translational terminator of yeast [47, 48, 49]. Hence, the aggregation of GFP-AnaA aided by Hsp42, Sis1 or Hsp104 was achieved through the process of inclusion formation and sequestration, but not through the process of refolding or disaggregation.

GVs are constituted from highly hydrophobic proteins that are challenging to purify and characterize. Correspondingly, the mechanism of their assembly, along with details of their supramolecular structure remained to be elucidated. It is instrumental to avoid misfolding and inappropriate aggregation of the GvpA, which may explain the presence of multiple accessory genes that putatively assist with assembly in their native operon [3, 27]. Previously, the GvpN is predicted to have a chaperone-like activity due to a possession of the ATPase domain [29]. In our study, GvpN is co-localized with GFP-AnaA aggregates and facilitates the inclusion formation of GFP-AnaA aggregates as well as their sequestration near the vacuole. To our best knowledge, this represents the first study on such a role of GvpN as a molecular chaperone. Given the positive roles of these chaperone proteins (Hsp42, Sis1, Hsp104, GvpN) in the GFP-AnaA aggregation, the co-expression of respective chaperone with GvpA is predicted to improve the GV assembly through maintaining a relatively higher cell viability, forming larger inclusion and enhancing sequestration of GvpA aggregates. Currently, we are in the process of verifying the improvement of GV assembly in the engineered yeast cells by tuning the expression of each of these chaperones.

4. Materials & Methods

4.1. Synthesis of cyanobacterial GV genes

Sequences of synthesized genes were listed in Table 1 and Table S1. AnaA, AnaC, PlaA and PlaC genes were synthesized with codon optimized for expression in *S. cerevisiae* by Integrated DNA Technologies (Integrated DNA Technologies, IA, USA).

4.2. Strains, plasmid and growth conditions

Yeast strain *Saccharomyces cerevisiae* BY4741 (*MATa leu2Δ0 met15Δ0 ura3Δ0 his3Δ1*) was used as the host for GV expression. *E. coli* DH5α was used for gene cloning and plasmid construction. Ampicillin and kanamycin were used at 100 μg/mL, 50 μg/ml, respectively. The engineered strains were grown in Synthetic Complete (SC) SC supplemented with glucose to a final concentration of 2% and dropout supplement lacking uracil (Sigma-Aldrich, MO, USA) were added when required. Primer sequences are listed in Table S2. A single colony was inoculated in 5 ml of SC-URA or SC media and cultured overnight. Cells were diluted to OD_{600} 0.2 with 50-100 ml of SC-URA or SC media and then incubated at 30°C at 220 rpm for indicated time.

4.3. Molecular cloning

All gas vesicle genes were synthesized and cloned by the Golden Gate assembly with modified YeastFab system [24]. The vector information for the insert and the accepting vector of the PART coning for each part of promoter, gene, and terminator, the POT cloning for constituting a single transcriptional unit (TU), MKU/CKU cloning for constituting multiple-transcriptional units, and the GAU for the genome integration vector were listed in the Table S2 and S3. The gBlock fragments of the gas vesicle genes were cloned via *Bsa*I (New England Biolabs, MA, USA) into the pHCK plasmid conferring kanamycin resistance. A transcriptional unit (TU) comprising of a promoter, a gas vesicle gene, and a terminator was assembled via an *Esp3*I (Thermo Fisher Scientific, MA, USA) into pPOT plasmids conferring Ampicillin resistance. The multiple TUs were cloned into the pMKU/pCKU vector conferring Kanamycin resistance using *Bsa*I. For the genome integration plasmid, the TU cloned into pGAU vector conferring Ampicillin resistance. The assembly was set up using 75 ng of each plasmid in a mix containing ligation butter, 10 U of the selected restriction enzyme (*Bsa*I or *Esp3*I) and 10 U of the T4 DNA ligase (Thermo Fisher Scientific, MA, USA), 0.5 × BSA in a final reaction volume of 10 µl. The reaction was incubated for 37 °C for 5 min, 16 °C for 5 min within 15 - 50 cycles and then 50 °C for 5 min and 80 °C for 5 min. All cloning was carried out using the *E. coli* TOP10. Designated plasmids were transformed into the *S. cerevisiae* (BY4741) using the LiAc/PEG method. Strains were listed in Table S4.

4.4. Gas vesicle protein expression and Western blot analysis

Five milliliters of overnight cultures of yeast strains in SC or SC-URA were diluted into 50 mL of fresh media and grown at 30°C as indicated. Total protein was extracted by using the lysis buffer (0.1 M NaOH, 2% beta-mercaptoethanol) [52]. The soluble part was taken after the centrifugation at 14,000 rpm for 10 min of the lysate and the pellets as the insoluble part was resuspended in 8 M urea. Protein concentration was measured by using the Pierce™ 660 nm Protein Assay Reagent (Thermo Fisher Scientific, MA, USA). Proteins were separated on the 12% Tricine-SDS-PAGE [53] and then transferred to the 0.45-µm pore nitrocellulose membrane (Bio-Rad laboratories, CA, USA) for 30 min at 25 V using the BioTrans-Blot Turbo System (Bio-Rad laboratories, CA, USA). The membrane was incubated for 1 h in blocking buffer (0.5% Non-fat dry milk) in TBS buffer containing 0.1 % Tween 20 (TBST), washed three times for 10 min in TBST buffer, and incubated

overnight at 4 °C with an HRP conjugated anti-HIS antibody diluted by 1:1000 (Thermo Fisher Scientific, MA, USA) in TBST buffer. The membrane was washed for three times using TBST buffer and developed using the Signal Fire ECL reagent (Cell Signaling Technology, MA, USA).

4.5. Yeast cell floating assay

Single colony was inoculated in 5 ml of SC-URA or SC media and cultured for overnight. The overnight culture was diluted to the OD_{600} 0.2 in 50 ml of SC media and then cultured at 30 °C at 220 rpm for indicated time (the 1st cultivation). At every time point, the 1st cultivation was adjusted to the OD_{600} 2.0 in 10 ml of the fresh medium in the 30 ml universal tube and then stationarily cultured for 1 d at 30 °C (the 2nd cultivation). The 2nd cultivation was completely resuspended and left at room temperature (RT) to observe the floating performance until the GVP strain and the WT control showed differential sedimentation.

4.6. GV isolation from yeast and cyanobacteria

Yeast cultures were pelleted and the cell wall was removed by the lyticase solution (50 mM Tris-HCl-pH 7.5, 5 mM $MgCl_2$, 1.4 M sorbitol, 0.5% beta-mercaptoethanol, and 300 U/ml lyticase) (Sigma-Aldrich, MO, USA) for 60 min at 25°C. Yeast protoplasts were lysed using the Y-PER™ Yeast Protein Extraction Reagent (Thermo Fisher Scientific, MA, USA) supplemented with final 10 μg/ml DNaseI (Sigma-Aldrich, MO, USA) and protease inhibitor (MedChemExpress, NJ, USA). GV fractions were separated from the lysate by the accelerated centrifugation at 300 g at 4 °C for 4 h. The supernatant including the white floated layer was carefully transferred to 2-ml tubes and processed by the accelerated centrifugation repeated for at least four times to isolate and enrich the white layer into the 10 mM Tris-HCl pH 7.5. The white layer sample was used for TEM analysis.

Cyanobacterial culture was collected, and GVs were isolated according to a previous study [25]. *Anabaena flos-aquae* (CCAP 1403/13F) and culture medium (BG-11 and JM solution) were purchased from CCAP (Culture Collection of Algae and Protozoa), and cyanobacterial cells were cultured at 25 °C, 100 rpm shaking under 14 h light- and 10 h dark-cycle. Once the culture reached to a dark green after around two weeks, GVs were extracted by hypertonic lysis with 500 mM sorbitol and 10% Solulyse (Genlantis, CA, US), and were purified by the accelerated centrifugation at 300g, repeatedly in 10 mM Tris-HCl-pH 7.5, followed by TEM observation.

446

447 4.8. Transmission Electron Microscopy

448 The isolated GVs were spotted on a Formvar/Carbon 200 mesh grid (Electron Microscopy
449 Science, UK) that was made hydrophilic by exposure to glow discharging for 20-s at 5 mA
450 (Leica, Germany). GV samples were negatively stained with 5% gadolinium triacetate
451 (Sigma-Aldrich, MO, USA) for 2 min. TEM observation was performed using a JEOL
452 1220 transmission electron microscope (JEOL USA Inc., MA, USA) equipped with a Gatan
453 digital camera (Gatan Inc., CA, USA). The dimension of GVs was measured by using
454 ImageJ (https://imagej.nih.gov).

455

456 4.9. Calcofluor white staining

457 A half milliliter of cultured cells was spun down, resuspend in 0.5 ml 1× PBS. Add 1 µl of
458 Calcofluor White M2R (Sigma-Aldrich, MO, USA) and incubated at 30 ºC for 10 min. The
459 cells (100 µl) in a 96-well plate were transferred into the well containing 100 µl of 1 × PBS
460 and then cells were serially diluted for 8 times at two-fold each time. Florescence intensity
461 was measured using a Tecan microplate reader (Perkin Elmer, MA, USA) at the wavelength
462 of 360 nm (excitation) and 460 nm (emission), respectively, and normalized to OD_{600}.

463

464 4.9. Semi-Denaturing Detergent-Agarose gel electrophoresis (SDD-AGE)

465 SDD-AGE was performed following the procedures described in a previous study [54]. Cells
466 were harvested, incubated in 1 ml of enzyme solution (50 mM Tris-HCl-pH 7.5, 5 mM
467 $MgCl_2$, 1.4 M sorbitol, 0.5% B-ME, and 300 U/ml lyticase) at 30°C for 1 h, and collected
468 by centrifugation at 800 g for 5 min at RT. The pellet was resuspended in 100 µl lysis
469 buffer (100 mM Tris-HCl-pH 7.5, 50 mM NaCl, and 10 ml B-ME, and Protease inhibitor)
470 and lysed with vortex for 2 min. The supernatant fraction was obtained by centrifugation at
471 4,000 g for 2 min, and mixed with sample buffer (2 × TAE, 20% glycerol, 8% SDS and
472 bromophenol blue) at a ratio of 1:4 (v/v). Agarose (1.5% w/v) containing 0.1% SDS was
473 used for gel electrophoresis in 1 × TAE buffer containing 0.1% SDS at 30 V for 360 -
474 420 min. Proteins were transferred onto a 0.45-µm pore nitrocellulose membrane (Bio-Rad
475 laboratories, CA, USA) based on a capillary transfer system. The membrane was incubated
476 for 1 h in blocking buffer (5% Non-fat dry milk in TBST), washed three times for 10 min in
477 TBST, and incubated overnight at 4°C with an HRP conjugated anti-GFP antibody diluted
478 by 1:1000 (v/v) (Thermo Fisher, MS, USA) in TBST buffer. The anti-PGK1 antibody used
479 for the internal control at a dilution of 1:1000 (v/v) (Abcam, UK). The membrane was

washed with TBST buffer for three times and developed with the Signal Fire ECL reagent (Cell Signaling Technology, MA, USA).

Supporting information

The following is available online. **Table S1**. A list of the codon optimized GVP gene sequences. **Table S2**. A list of primers used in this study**. Table S3**. A list of plasmids and inserts for the YeastFab-based cloning. **Table S4**. A list of the strains used in this study**. Figure S1**. Schematic representation of the strategy for the genetic reconstitution of GVs in yeast *S. cerevisiae* and amino acid sequences of GvpA and GvpC from *Anabaena flos-aquae* (Ana) and *Planktothrix rucescens* (Pla). **Figure S2**. GVP expression in plasmids carrying four combinations of GvpA and GvpC genes in yeast cells. **Figure S3**. Growth profile and expressions of GvpG and GvpC genes with genome-integration in yeast cells.

Acknowledgments

This research was funded by the Start-up Grant (NUHSRO/2016/099/SU/01), Synthetic Biology Translational Research Programme (NUHSRO/2020/077/MSC/02/SB) of the Yong Loo Lin School of Medicine, National University of Singapore, and the Industry Alignment Fund-Industry Collaboration Project (ICP1600012) of the Agency for Science, Technology and Research (A*STAR), Singapore. We thank Mr. Lu Thong Beng in the NUS Electron Microscopy Unit (EMU) for the advice on TEM analysis, and Dr. Roopa Rajashekar for the comments made to the manuscript.

Conflict of Interest

The authors declare no commercial or financial conflict of interest.

Author Contribution

H.J., N.H.C. and M.W.C. designed the study. H.J. performed experiments. Y.Q.T. assisted in molecular cloning. H.J. wrote the manuscript. H.L., W.S.Y., M.W.C., and N.H.C reviewed the manuscript. W.S.Y., M.W.C., and N.H.C. supervised this project. All authors have read and agreed to the published version of the manuscript.

References

[1] Walsby, A. E. Gas Vesicles. *Microbiol. Mol. Biol. Rev.* **1994**, *58*, 94–144.

[2] Strunk, T.; Hamacher, K.; Hoffgaard, F.; Engelhardt, H.; Zillig, M. D.; Faist, K.; Wenzel, W.; Pfeifer, F. Structural Model of the Gas Vesicle Protein GvpA and Analysis of GvpA Mutants in Vivo. *Mol. Microbiol.* **2011**, *81*, 56–68; doi.org/10.1111/j.1365-2958.2011.07669.x.

[3] Bayro, M. J.; Daviso, E.; Belenky, M.; Griffin, R. G.; Herzfeld, J. An Amyloid Organelle, Solid-State NMR Evidence for Cross-β Assembly of Gas Vesicles. *J. Biol. Chem.* **2012**, *287*, 3479–3484; doi.org/10.1074/jbc.M111.313049.

[4] Pancrace C,; Barny MA,; Ueoka R, Calteau A,; Scalvenzi T,; Pédron J,; Barbe V,; Piel J,; Humbert JF,; Gugger M. Insights into the Planktothrix genus: Genomic and metabolic comparison of benthic and planktic strains. *Sci. Rep.* **2017**, *7*, 41181; doi.org/10.1038/srep41181

[5] Walsby, A. E.; Hayes, P. K. The Minor Cyanobacterial Gas Vesicle Protein, GVPc, Is Attached to the Outer Surface of the Gas Vesicle. *Microbiol.* **1988**, *134*, 2647–2657; doi.org/10.1099/00221287-134-10-2647.

[6] Walsby, A. E.; Iglesias-Rodríguez, D.; Davis, P. A.; Skulberg, O. M.; Beard, S. J. Gas Vesicle Genes in Planktothrix Spp. from Nordic Lakes: Strains with Weak Gas Vesicles Possess a Longer Variant of GvpC. *Microbiol.* **2000**, *146*, 2009–2018; doi.org/10.1099/00221287-146-8-2009.

[7] Shapiro, M. G.; Goodwill, P. W.; Neogy, A.; Yin, M.; Foster, F. S.; Schaffer, D. V.; Conolly, S. M. Biogenic Gas Nanostructures as Ultrasonic Molecular Reporters. *Nat. Nanotechnol.* **2014**, *9* , 311–316; doi.org/10.1038/nnano.2014.32.

[8] Shapiro, M. G.; Ramirez, R. M.; Sperling, L. J.; Sun, G.; Sun, J.; Pines, A.; Schaffer, D. V.; Bajaj, V. S. Genetically Encoded Reporters for Hyperpolarized Xenon Magnetic Resonance Imaging. *Nat. Chem.* **2014**, *6*, 629–634; doi.org/10.1038/nchem.1934.

[9] Bourdeau, R. W.; Lee-Gosselin, A.; Lakshmanan, A.; Farhadi, A.; Kumar, S. R.; Nety, S. P.; Shapiro, M. G. Acoustic Reporter Genes for Noninvasive Imaging of Microorganisms in Mammalian Hosts. *Nature* **2018**, *553*, 86–90; doi.org/10.1038/nature25021.

[10] Farhadi, A.; Ho, G. H.; Sawyer, D. P.; Bourdeau, R. W.; Shapiro, M. G. Ultrasound Imaging of Gene Expression in Mammalian Cells. *Science* **2019**, *365*, 1469–1475; doi.org/10.1126/science.aax4804.

[11] Wang, T.; Kang, L.; Li, J.; Wu, W.; Zhang, P.; Gong, M.; Lai, W.; Zhang, C.; Chang, L.; Peng, Y.; Yang, Z.; Li, L.; Bao, Y.; Xu, H.; Zhang, X.; Sui, Z.; Yang, G.; Wang, X. Floating Escherichia Coli by Expressing Cyanobacterial Gas Vesicle Genes. *J. Ocean Univ. China* **2015**, *14*, 84–88; doi.org/10.1007/s11802-015-2344-3.

[12] Mizushima, R.; Inoue, K.; Fujiwara, H.; Iwane, A.H.; Watanabe, T.M.; Kimura, A. Multiplexed 129Xe HyperCEST MRI Detection of Genetically Reconstituted Bacterial Protein Nanoparticles in Human Cancer Cells. *Contrast Media Mol. Imaging* **2020**, *2020*, 5425934; doi:10.1155/2020/5425934.

[13] Escusa-Toret, S.; Vonk, W.I.M.; Frydman, J. Spatial sequestration of misfolded proteins by a dynamic chaperone pathway enhances cellular fitness during stress. *Nat. Cell Biol.* **2013**, *15*, 1231–1243; doi:10.1038/ncb2838.

[14] Sivertsen, A. C.; Bayro, M. J.; Belenky, M.; Griffin, R. G.; Herzfeld, J. Solid-State NMR Characterization of Gas Vesicle Structure. *Biophys. J.* **2010**, *99* , 1932–1939; doi.org/10.1016/j.bpj.2010.06.041.

[15] Wetzel, R. Mutations and Off-Pathway Aggregation of Proteins. *Trends Biotechnol.* **1994**, *12*, 193–198; doi.org/10.1016/0167-7799(94)90082-5.

[16] Landreh, M.; Sawaya, M. R.; Hipp, M. S.; Eisenberg, D. S.; Wüthrich, K.; Hartl, F. U. The Formation, Function and Regulation of Amyloids: Insights from Structural Biology. *J. Intern. Med.* **2016**, *280*, 164–176; doi.org/10.1111/joim.12500.

[17] Hill, S. M.; Hanzén, S.; Nyström, T. Restricted Access: Spatial Sequestration of Damaged Proteins during Stress and Aging. *EMBO. Rep.* **2017**, *18*, 377–391; doi.org/10.15252/embr.201643458.

[18] Labbadia, J.; Morimoto, R. I. The Biology of Proteostasis in Aging and Disease. *Annu. Rev. Biochem.* **2015**, *84*, 435–464; doi.org/10.1146/annurev-biochem-060614-033955.

[19] Mogk, A.; Bukau, B.; Kampinga, H. H. Cellular Handling of Protein Aggregates by Disaggregation Machines. *Mol. Cell* **2018**, *69*, 214–226; doi.org/10.1016/j.molcel.2018.01.004.

[20] Bracher, A.; Verghese, J. The Nucleotide Exchange Factors of Hsp70 Molecular Chaperones. *Front. Mol. Biosci.* **2015**, *2*. 10; doi.org/10.3389/fmolb.2015.00010.

[21] Glover, J. R.; Lindquist, S. Hsp104, Hsp70, and Hsp40: A Novel Chaperone System That Rescues Previously Aggregated Proteins. *Cell* **1998**, *94*, 73–82; doi.org/10.1016/S0092-8674(00)81223-4.

[22] Čiplys, E.; Aučynaitė, A.; Slibinskas, R. Generation of Human ER Chaperone BiP in Yeast Saccharomyces Cerevisiae. *Microb. Cell Fact.* **2014**, *13*, 22; doi.org/10.1186/1475-2859-13-22.

[23] Shen, Q.; Wu, M.; Wang, H.-B.; Naranmandura, H.; Chen, S.-Q. The Effect of Gene Copy Number and Co-Expression of Chaperone on Production of Albumin Fusion Proteins in Pichia Pastoris. *Appl. Microbiol. Biotechnol.* **2012**, *96*, 763–772; doi.org/10.1007/s00253-012-4337-0.

[24] Guo, Y.; Dong, J.; Zhou, T.; Auxillos, J.; Li, T.; Zhang, W.; Wang, L.; Shen, Y.; Luo, Y.; Zheng, Y.; Lin, J.; Chen, G.-Q.; Wu, Q.; Cai, Y.; Dai, J. YeastFab: The Design and Construction of Standard Biological Parts for Metabolic Engineering in *Saccharomyces Cerevisiae*. *Nucleic Acids Res.* **2015**, *43*, e88–e88; doi.org/10.1093/nar/gkv464.

[25] Lakshmanan, A.; Lu, G. J.; Farhadi, A.; Nety, S. P.; Kunth, M.; Lee-Gosselin, A.; Maresca, D.; Bourdeau, R. W.; Yin, M.; Yan, J.; Witte, C.; Malounda, D.; Foster, F. S.; Schröder, L.; Shapiro, M. G. Preparation of Biogenic Gas Vesicle Nanostructures for Use as Contrast Agents for Ultrasound and MRI. *Nat. Protoc.* **2017**, *12*, 2050–2080; doi.org/10.1038/nprot.2017.081.

[26] Walsby, A. E. Structure and Function of Gas Vacuoles. *Bacteriol. Rev.* **1972**, *36* , 1–32.; doi.org/10.1128/MMBR.36.1.1-32.1972.

[27] Pfeifer, F. Distribution, Formation and Regulation of Gas Vesicles. *Nat. Rev. Microbiol.* **2012**, *10* , 705–715; doi.org/10.1038/nrmicro2834.

[28] Stagoj, M. N.; Komel, R.; Comino, A. Microtiter Plate Assay of Yeast Cell Number Using the Fluorescent Dye Calcofluor White M2R. *BioTechniques* **2004**, *36*, 380–382; doi.org/10.2144/04363BM01.

[29] Snider, J.; Houry, W. A. MoxR AAA+ ATPases: A Novel Family of Molecular Chaperones? *J. Struct. Biol.* **2006**, *156*, 200–209; doi.org/10.1016/j.jsb.2006.02.009.

[30] Offner, S.; Hofacker, A.; Wanner, G.; Pfeifer, F. Eight of Fourteen Gvp Genes Are Sufficient for Formation of Gas Vesicles in Halophilic Archaea. *J. Bacteriol.* **2000**, *182*, 4328–4336; doi.org/10.1128/jb.182.15.4328-4336.2000.

[31] Li, N.; Cannon, M. C. Gas Vesicle Genes Identified in Bacillus Megaterium and Functional Expression in Escherichia Coli. *J Bacteriol* **1998**, *180*, 2450–2458; doi:10.1128/JB.180.9.2450-2458.1998

[32] Fink, A. L. Protein Aggregation: Folding Aggregates, Inclusion Bodies and Amyloid. *Fold. Des.* **1998**, *3*, R9–R23; doi.org/10.1016/S1359-0278(98)00002-9.

[33] Hipp, M. S.; Kasturi, P.; Hartl, F. U. The Proteostasis Network and Its Decline in Ageing. *Nat. Rev. Mol. Cell Biol.* **2019**, *20*, 421–435; doi.org/10.1038/s41580-019-0101-y.

[34] Marshall, K. E.; Marchante, R.; Xue, W.-F.; Serpell, L. C. The Relationship between Amyloid Structure and Cytotoxicity. *Prion* **2014**, *8*, 192–196; doi.org/10.4161/pri.28860.

[35] Baldwin, W. W.; Kubitschek, H. E. Buoyant Density Variation during the Cell Cycle of Saccharomyces Cerevisiae. *J. Bacteriol.* **1984**, *158*, 701–704; doi.org/10.1128/JB.158.2.701-704.1984.

[36] deSousa, S. R.; Oliveira, K. F.; Souza, C. S.; Kilikian, B. V.; Laluce, C. Yeast Flotation Viewed as the Result of the Interplay of Supernatant Composition and Cell-Wall Hydrophobicity. *Colloids Surf. B Biointerfaces* **2003**, *29*, 309–319; doi.org/10.1016/S0927-7765(03)00019-5.

[37] Stewart, G. Yeast Flocculation—Sedimentation and Flotation. *Fermentation* **2018**, *4*, 28; doi.org/10.3390/fermentation4020028.

[38] Beard, S. J.; Davis, P. A.; Iglesias-Rodrı Guez, D.; Skulberg, O. M.; Walsby, A. E. Gas Vesicle Genes in Planktothrix Spp. from Nordic Lakes: Strains with Weak Gas Vesicles Possess a Longer Variant of GvpC. *Microbiology (Reading, Engl.)* **2000**, *146 (Pt 8)*, 2009–2018; doi.org/10.1099/00221287-146-8-2009.

[39] Ginzberg, M. B.; Kafri, R.; Kirschner, M. On Being the Right (Cell) Size. *Science* **2015**, *348*; doi.org/10.1126/science.1245075.

[40] Neurohr, G. E.; Terry, R. L.; Lengefeld, J.; Bonney, M.; Brittingham, G. P.; Moretto, F.; Miettinen, T. P.; Vaites, L. P.; Soares, L. M.; Paulo, J. A.; Harper, J. W.; Buratowski, S.; Manalis, S.; Werven, F. J. van; Holt, L. J.; Amon, A. Excessive Cell Growth Causes Cytoplasm Dilution And Contributes to Senescence. *Cell* **2019**, *176*, 1083-1097.e18; doi.org/10.1016/j.cell.2019.01.018.

[41] Steinkraus, K. a.; Kaeberlein, M.; Kennedy, B. k. Replicative Aging in Yeast: The Means to the End. *Annu. Rev. Cell Dev. Biol.* **2008**, *24*, 29–54; doi.org/10.1146/annurev.cellbio.23.090506.123509.

[42] Tyedmers, J.; Mogk, A.; Bukau, B. Cellular Strategies for Controlling Protein Aggregation. *Nat. Rev. Mol. Cell. Biol.* **2010**, *11*, 777–788; doi.org/10.1038/nrm2993.

[43] Yang, J.; Dungrawala, H.; Hua, H.; Manukyan, A.; Abraham, L.; Lane, W.; Mead, H.; Wright, J.; Schneider, B. L. Cell Size and Growth Rate Are Major Determinants of Replicative Lifespan. *Cell Cycle* **2011**, *10*, 144–155; doi.org/10.4161/cc.10.1.14455.

[44] Hartl, F. U.; Bracher, A.; Hayer-Hartl, M. Molecular Chaperones in Protein Folding and Proteostasis. *Nature* **2011**, *475*, 324–332; doi.org/10.1038/nature10317.

[45] Specht, S.; Miller, S. B. M.; Mogk, A.; Bukau, B. Hsp42 Is Required for Sequestration of Protein Aggregates into Deposition Sites in Saccharomyces Cerevisiae. *J. Cell Biol.* **2011**, *195*, 617–629; doi.org/10.1083/jcb.201106037.

[46] Haslbeck, M.; Braun, N.; Stromer, T.; Richter, B.; Model, N.; Weinkauf, S.; Buchner, J. Hsp42 Is the General Small Heat Shock Protein in the Cytosol of Saccharomyces Cerevisiae. *EMBO J.* **2004**, *23*, 638–649; doi.org/10.1038/sj.emboj.7600080.

[47] Chernoff, Y. O.; Lindquist, S. L.; Ono, B.; Inge-Vechtomov, S. G.; Liebman, S. W. Role of the Chaperone Protein Hsp104 in Propagation of the Yeast Prion-like Factor [Psi+]. *Science* **1995**, *268*, 880–884; doi.org/10.1126/science.7754373.

[48] Astor, M. T.; Kamiya, E.; Sporn, Z. A.; Berger, S. E.; Hines, J. K. Variant-Specific and Reciprocal Hsp40 Functions in Hsp104-Mediated Prion Elimination. *Mol. Microbiol.* **2018**, *109*, 41–62; doi.org/10.1111/mmi.13966.

[49] Greene, L. E.; Zhao, X.; Eisenberg, E. Curing of [PSI+] by Hsp104 Overexpression: Clues to Solving the Puzzle. *Prion* **2018**, *12*, 9–15; doi.org/10.1080/19336896.2017.1412911.

[50] Xu, B.-Y.; Dai, Y.-N.; Zhou, K.; Liu, Y.-T.; Sun, Q.; Ren, Y.-M.; Chen, Y.; Zhou, C.-Z. Structure of the Gas Vesicle Protein GvpF from the Cyanobacterium Microcystis Aeruginosa. *Acta Crystallogr D Biol. Crystallogr.* **2014**, *70*, 3013–3022; doi.org/10.1107/S1399004714021312.

[51] Tavlaridou, S.; Winter, K.; Pfeifer, F. The Accessory Gas Vesicle Protein GvpM of Haloarchaea and Its Interaction Partners during Gas Vesicle Formation. *Extremophiles* **2014**, *18* , 693–706; doi.org/10.1007/s00792-014-0650-0.

[52] Chen, B.; Ling, H.; Chang, M. W. Transporter Engineering for Improved Tolerance against Alkane Biofuels in Saccharomyces Cerevisiae. *Biotechnol. Biofuels* **2013**, *6*, 21; doi.org/10.1186/1754-6834-6-21.

[53] Schägger, H. Tricine-SDS-PAGE. *Nat. Protoc.* **2006**, *1*, 16–22; doi.org/10.1038/nprot.2006.4.

[54] Halfmann, R.; Lindquist, S. Screening for Amyloid Aggregation by Semi-Denaturing Detergent-Agarose Gel Electrophoresis. *J. Vis. Exp.* **2008**, *17*, e838; doi.org/10.3791/838.